Astron. Astrophys. 354, 1014–1020 (2000)

ASTRONOMY AND ASTROPHYSICS

# A wind accretion wake in RW Hydrae?⋆

**T. Dumm**[1], **D. Folini**[2], **H. Nussbaumer**[1], **H. Schild**[1], **W. Schmutz**[1,3], **and R. Walder**[1]

[1] Institute of Astronomy, ETH-Zentrum, 8092 Zürich, Switzerland
[2] Institute of Applied Mathematics, ETH-Zentrum, 8092 Zürich, Switzerland
[3] PMOD/WRC, 7260 Davos-Dorf, Switzerland

Received 18 October 1999 / Accepted 7 January 2000

**Abstract.** RW Hydrae is an eclipsing detached binary star system, consisting of a mass losing M-giant and a hot white dwarf on circular orbits. We analyze UV observations of RW Hydrae. Approximately at $\phi = 0.78$, clearly unrelated to the primary eclipse, we detect in the UV light curve an event with significantly reduced UV flux. The spectral characteristics of this event indicate Rayleigh scattering due to a high column density of neutral hydrogen in the line of sight to the hot white dwarf.

We model this observation in the framework of an accretion wake trailing the white dwarf. This interpretation is analogous to comparable models for $\zeta$ Aur systems and X-ray binaries. We find qualitative agreement between our 3D hydrodynamical accretion simulation and the observed UV light curve of RW Hya.

**Key words:** accretion, accretion disks – hydrodynamics – stars: winds, outflows – stars: binaries: close – stars: binaries: eclipsing – stars: individual: RW Hya

## 1. Introduction

Accretion phenomena are of relevance in a wide range of astrophysical objects. Here we consider the case of wind accretion within a binary system, where the mass losing object is smaller than its Roche lobe. If the relative velocity between the accretor and the medium is supersonic, a shock front forms around the accreting star. This shock front limits the accretion wake, a region of highly increased density.

Observational signs for accretion wakes were reported in $\zeta$ Aur systems and X-ray binaries. For Cen X–3 (Pounds et al. 1975) and Vela X–1 (Watson & Griffiths 1977) minima in the X-ray light curve out of eclipse have been found. Jackson (1975) presented a simple model, where such a luminosity decrease was attributed to a dense accretion wake trailing the neutron star. Kaper et al. (1994) and Feldmeier et al. (1996) later realized the importance of the termination of the radiative force driving the wind of the primary as the wind enters the highly ionized region around the neutron star. $\zeta$ Aur systems consist of a mass losing cool supergiant and a hot main sequence star. In these systems the light of the hot star probes the absorption column as a function of phase. Extended UV observations with IUE (International Ultraviolet Explorer) have provided evidence for accretion wakes in $\zeta$ Aur (Chapman 1981), 22 Vul (Ahmad & Parsons 1985), 32 Cyg (Ahmad 1986), 31 Cyg (Ahmad 1989) and AL Vel (Eaton 1994).

The eclipsing symbiotic binary RW Hya is a detached system consisting of a non-pulsating mass losing M-giant and a hot white dwarf on circular orbits with a period of $370$ days (Schild et al. 1996; Kenyon & Mikolajewska 1995). Thus, we are looking at a system where wind accretion onto a white dwarf is possibly going on. Wind accretion is thought to be a necessary condition for the occurrence of symbiotic novae, however, up to now it has not been directly observed.

In this Paper we present observational evidence suggesting that the white dwarf in RW Hya is trailed by an accretion wake. In Sect. 2 we compile the available UV data of the system. In Sect. 3, we analyze the UV light curve which reveals at $\phi = 0.78$ a high column density in the line of sight to the white dwarf. We associate this with wind accretion on the white dwarf. A wind or the radiation field from the white dwarf could prevent accretion. In Sect. 4 we put an upper limit on a radiation driven wind from the hot white dwarf in RW Hya. In Sect. 5 we present a hydrodynamical accretion simulation, which we compare in Sect. 6 with the observed light curve.

## 2. UV observations

RW Hya has been observed at various orbital phases with IUE. It has also been observed at three orbital phases with the Goddard High Resolution Spectrograph (GHRS) of the Hubble Space Telescope (HST). A log of all IUE low resolution large aperture observations is given in Kenyon & Mikolajewska (1995). For this work, we employ all available, non-saturated IUE low resolution large aperture spectra. In Table 1 we give the average continuum flux in the interval between $1250$ Å and $1290$ Å, hereafter called $F(\lambda 1270)$.

*Send offprint requests to*: T. Dumm

⋆ Based on observations with the International Ultraviolet Explorer and observations with the NASA/ESA Hubble Space Telescope, obtained at the Space Telescope Science Institute, which is operated by the Association of Universities for Research in Astronomy, Inc. under NASA contract No. NAS5-26555.

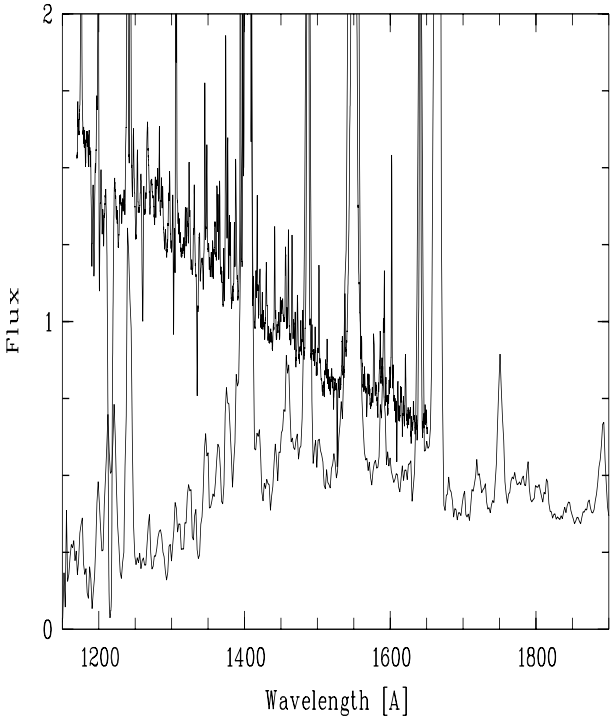


**Fig. 1.** IUE and HST GHRS UV spectra of RW Hya. Upper spectrum taken at $\phi = 0.71$ (HST). Lower spectrum taken at $\phi = 0.78$ (IUE) showing the effect of Rayleigh scattering due to a high column density of neutral hydrogen. Flux in units of $10^{-12}$ erg/(cm$^2$ s Å).

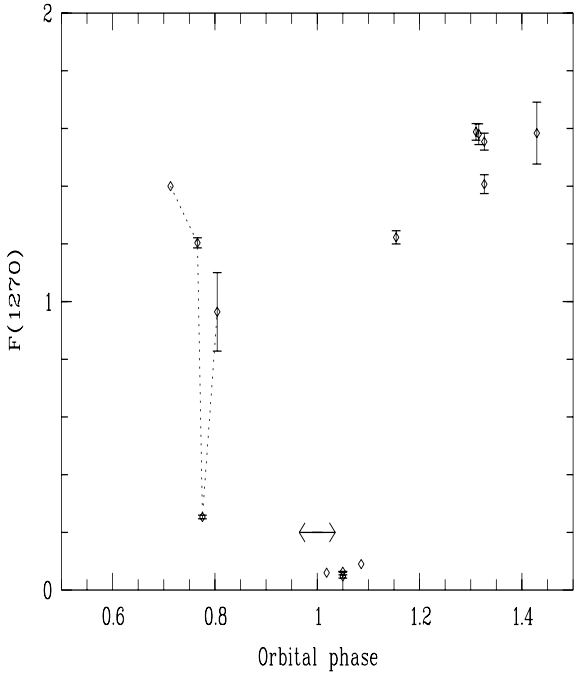


**Fig. 2.** Flux variation in RW Hya at 1270 Å , in units of $10^{-12}$ erg/(cm$^2$ s Å). The horizontal arrow marks the range where the M-giant geometrically occults the white dwarf. The error bars of the three HST measurements have significantly smaller error bars than the IUE data, and are not plotted. For clarity a dotted line connecting the measurements around $\phi = 0.75$ is plotted.

**Table 1.** RW Hya continuum flux variation at $\lambda 1270$ as measured in the 10 IUE low resolution spectra and the 3 HST low resolution spectra after convolving them down to IUE low resolution. Flux in units of $10^{-14}$ erg cm$^{-2}$ s$^{-1}$ Å$^{-1}$.

| Date | JD | $\phi$ | $F(\lambda 1270)$ |
|---|---|---|---|
| 1979, Jan 2 | 2 443 876 | 0.78 | 25 |
| 1979, July 19 | 2 444 074 | 0.31 | 159 |
| 1979, July 21 | 2 444 076 | 0.32 | 158 |
| 1979, July 25 | 2 444 080 | 0.33 | 148 |
| 1979, Sep 1 | 2 444 118 | 0.43 | 158 |
| 1980, Jan 17 | 2 444 257 | 0.81 | 96 |
| 1981, Jan 8 | 2 444 613 | 0.77 | 120 |
| 1985, June 21 | 2 446 238 | 0.15 | 122 |
| 1987, May 24 | 2 446 940 | 0.05 | 6 |
| 1996, Mar 5 | 2 450 148 | 0.71 | 140 |
| 1996, June 26 | 2 450 261 | 0.02 | 6 |
| 1996, July 21 | 2 450 286 | 0.09 | 9 |

A log of the available HST GHRS observations is given in Dumm et al. (1999). Here we use all the GHRS low resolution spectra and we analyze the medium resolution spectrum of N V $\lambda 1239, 1243$ for signatures of a stellar wind (Sect. 4).

The orbital phase $\phi$ for a given Julian date is taken from the ephemeris of Kenyon & Mikolajewska (1995) and Schild et al. (1996). Both ephemeris are based on radial velocity measurements derived from M-star spectra, and are in very good agreement. We take the average of the two solutions:

$$\phi = (JD - 2\,445\,070) \,/\, 370.3 \qquad (1)$$

The phase $\phi = 0$ corresponds to mid-eclipse of the white dwarf by the M-giant.

## 3. Observed UV light curve

Below 1600 Å the observed continuum flux is dominated by radiation from the white dwarf. Shortly before and after geometric eclipse by the M-giant, the white dwarf continuum is strongly attenuated. The spectral characteristic of the flux reduction indicates Rayleigh scattering by neutral hydrogen in the M-giant wind and line blanketing by Fe II absorption lines (Dumm et al. 1999; see also Vogel 1991; Shore & Aufdenberg 1993). In addition to the attenuation close to the photospheric eclipse by the M-giant, RW Hya shows this phenomenon also at $\phi = 0.78$, when the binary system is approximately at quadrature. In Fig. 1 we compare the IUE spectrum taken at this phase with the unaffected spectrum at phase $\phi = 0.71$ obtained with HST. The strength of the attenuation requires a column density of neutral hydrogen of $\approx 10^{23}$ cm$^{-2}$.

The flux variation $F(\lambda 1270)$, where Rayleigh scattering is the dominant attenuation source, is shown in Fig. 2. At phases $\phi = 0.77$ and 0.81 we still detect weak attenuation but the spectrum taken at $\phi = 0.71$ is not affected. The flux reduction

at quadrature lasts thus for $\Delta\phi \approx 0.04$, and is well isolated from the normal photospheric eclipse by the M-giant. The orbit of RW Hya is known accurately, we therefore exclude significant errors in the phases.

In Sect. 5 we shall model this observational finding with an accretion wake trailing the white dwarf. A necessary requirement for such a model to be appropriate is that the white dwarf radiation field cannot prevent accretion, and that the white dwarf has no significant wind.

## 4. Limits for a white dwarf wind

For winds from the hot component in symbiotic binaries, qualitatively different results have been found for different systems. In AG Peg a strong P Cygni profile in N V $\lambda\lambda 1239, 1243$ reveals the existence of a white dwarf wind with a terminal velocity of $v_\infty^{\rm h} \approx 1000\ {\rm km\,s^{-1}}$ (Nussbaumer et al. 1995). The spectrum of AG Peg has been analyzed by Schmutz (1996), who derived a mass-loss rate of $\dot{M}_{\rm h} = 10^{-6.7}\ {\rm M_\odot/yr}$. For EG And Vogel (1993) found $v_\infty^{\rm h} \approx 500\ {\rm km\,s^{-1}}$ and $\dot{M}_{\rm h} \approx 5 \cdot 10^{-9}\ {\rm M_\odot}$. For RR Tel no trace of a wind from the hot component can be found in HST GHRS spectra (Nussbaumer & Dumm 1997). For the eclipsing symbiotic nova PU Vul, a white dwarf wind with $v_\infty^{\rm h} \approx 1\,000\,{\rm km\,s^{-1}}$ has been detected in the N V $\lambda\lambda 1239, 1243$ emission line (Nussbaumer & Vogel 1996). In Fig. 3 we compare the N V $\lambda\lambda 1239, 1243$ line profile of RW Hya taken at $\phi = 0.71$, with that of AG Peg. In AG Peg the P Cygni profile corresponds to $1\,000\ {\rm km\,s^{-1}}$. In the spectrum of RW Hya we see a P Cygni absorption feature corresponding to $\approx 100$ km/s, but there is no indication for a P Cygni absorption from a faster wind.

With the wind momentum-luminosity relation (WLR) for radiation driven winds (Kudritzki 1998) we can calculate a mass-loss rate $\dot{M}_{\rm h}$ for the white dwarf. The luminosity of the white dwarf in RW Hya has been determined by Kenyon & Mikolajewska (1995) and Schild et al. (1996). Inserting the upper limit given by Schild et al. (1996), $L_{\rm h} < 1200\ {\rm L_\odot}$, into the WLR leads to a mass-loss rate $\dot{M}_{\rm h} \lesssim 3 \cdot 10^{-9}\ {\rm M_\odot/yr}$. The lower value of Kenyon & Mikolajewska (1995), $L_{\rm h} = 160\ {\rm L_\odot}$, corresponding to a distance of $0.67$ kpc derived by Schild et al. (1996) yields $\dot{M}_{\rm h} \approx 10^{-10}\ {\rm M_\odot/yr}$. Both groups find a similar white dwarf radius, $R_{\rm h} \approx 0.04\ {\rm R_\odot}$. Schild et al. (1996) derived a white dwarf mass of $0.5{\rm M_\odot}$. This leads to an escape velocity of $v_{\rm esc} \approx 2000\ {\rm km\ s^{-1}}$. Typically, the terminal velocities of the winds of central stars of planetary nebulae (CSPN) are about 2.5 times the escape velocity, indicating for RW Hya $v_\infty^{\rm h} \approx 5\,000\ {\rm km\ s^{-1}}$.

One has to keep in mind, that the observed properties of winds from the hot components in AG Peg, EG And, and PU Vul strongly differ from those predicted by the WLR. This might be due to the large extrapolation, as the least luminous objects used to derive the WLR have luminosisties $\gtrsim 1\,000\ {\rm L_\odot}$ and temperatures $\lesssim 100\,000$ K.

In order to test whether a possible white dwarf wind is significant compared to the red giant wind, we have to compare the momentum fluxes of the two winds. Along the binary axis they are balanced at a distance $r$ from the white dwarf

$$\frac{r}{s} = \left(1 + \sqrt{\frac{\dot{M}_{\rm r}\, v_\infty^{\rm r}}{\dot{M}_{\rm h}\, v_\infty^{\rm h}}}\right)^{-1}, \qquad (2)$$

where $s$ is the binary separation.

A hot wind velocity of $v_\infty^{\rm h} = 5\,000\ {\rm km\,s^{-1}}$, together with $\dot{M}_{\rm h} = 10^{-10}\ {\rm M_\odot/yr}$, $\dot{M}_{\rm r} = 10^{-7}\ {\rm M_\odot/yr}$ and $v_\infty^{\rm r} = 20\ {\rm km\,s^{-1}}$, leads to $r/s \approx 0.3$ corresponding to $\approx 80\ {\rm R_\odot}$. We will discuss the implications of a wind from the white dwarf in Sect. 6.

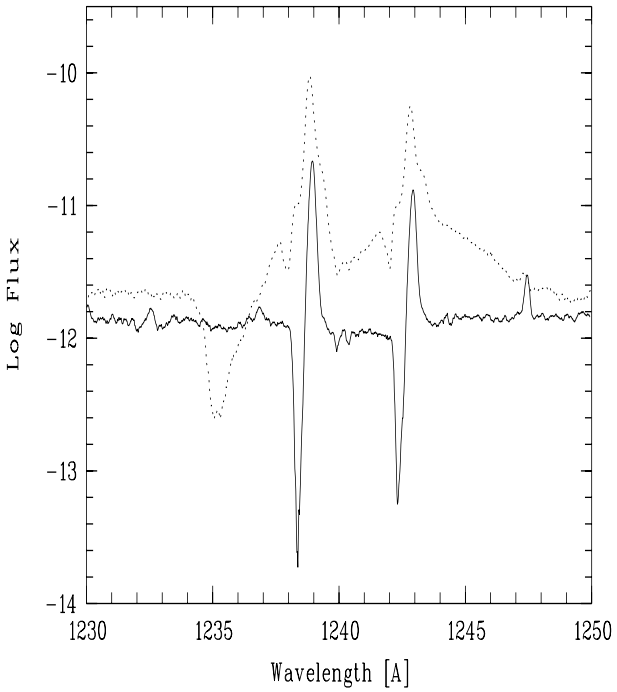


**Fig. 3.** The P Cygni profile in the N V $\lambda\lambda 1239, 1243$ Å doublet of AG Peg (dotted) indicates a fast wind with a 'zero' intensity expansion velocity (Howarth & Prinja 1989) $v_\infty \approx 1000\ {\rm km\,s^{-1}}$, and an absorption feature corresponding to $\approx 200\ {\rm km\,s^{-1}}$. The RW Hya spectrum (solid) shows only the absorption feature at $\approx 100\ {\rm km\,s^{-1}}$. Both spectra have been corrected for the system velocity, the flux is in units of erg/(cm$^2$ s Å).

## 5. Accretion models

Early analytical accretion models by Hoyle & Lyttleton (1939) and Bondi & Hoyle (1944) dealt with homogeneous, uniform flows interacting with an accreting sphere. In recent years numerical simulations by various authors have basically confirmed these analytical results (e.g. Ruffert 1996 and references therein). These studies can be directly applied to situations, where the Bondi-Hoyle accretion radius,

$$R_{\rm BH} = 2\,G\,M\,/\,v_\infty^2, \qquad (3)$$

is small compared to distances over which density and velocity gradients in the stellar wind are significant ($M$ is the mass of

the accretor, $G$ the gravitational constant, and $v_\infty$ the relative velocity of the medium far away from the accretor). For evolved low mass binary systems, like s-type symbiotics or $\zeta$ Aurigae systems, this condition is not fulfilled, as for these systems $R_{\rm BH} \approx 500\,{\rm R}_\odot$. Several hydrodynamical simulations for $\zeta$ Aur and symbiotic binary systems have been performed, e.g. Theuns & Jorissen (1993), Bisikalo et al. (1995), Theuns et al. (1996), Walder (1997), and Mastrodemos & Morris (1998). These simulations found that the accretion rate is significantly lower than predicted by the Bondi-Hoyle-Lyttleton formula, and that the accretion wake is spiral–shaped. In the following we model the occultation seen in RW Hya around $\phi = 0.78$ in terms of wind accretion.

### *5.1. Model assumptions*

The velocity and density distribution of the unperturbed M-giant wind inside the accretion radius of the white dwarf determines the orientation of the accretion wake. The M-giant wind law $v(r)$ of SY Mus (Dumm et al. 1999) suggests that the M-giant wind expands at negligible velocities until it reaches a stellar distance of $\approx 2.5$ M-giant radii. At $\approx 2.5 \cdot R_{\rm r}$ the wind is then strongly accelerated. The accretion geometry is thus strongly influenced by the M-giant wind acceleration. At present the mechanism of wind formation in non-pulsating M-giants is very poorly known. Radiation pressure on dust grains is important, but it will only act beyond several stellar radii from the M-giant, where dust formation starts (Danchi et al. 1994). The mechanism which brings the wind material to the condensation distance is not known.

For our hydrodynamical simulation we therefore represent the M-giant wind in the following simplified way: Similarly to Theuns & Jorissen (1993) we assume that at any point non-thermal wind driving forces are balanced by gravitation of the M-giant. The forces acting on the M-giant wind are thus gravitation due to the white dwarf, and forces due to gas pressure gradients. Around the accretor the unperturbed wind velocity, $v(r/R_{\rm r})$, then behaves like

$$v(r/R_{\rm r}) \approx 2\, v_{\rm sound} \sqrt{\ln\,(r/R_{\rm r})}. \qquad (4)$$

Our wind velocity law is slightly steeper than the one of Mastrodemos & Morris (1998) who performed 3D SPH accretion simulations of detached binary systems containing a mass losing AGB star.

All the parameters entering the numerical simulation are listed in Table 2. In our calculation the M-giant wind is allowed to accelerate from a sphere with radius $R_{\rm r}^{\rm c} = 2.5 \cdot R_{\rm r} = 150\,{\rm R}_\odot$ (Schild et al. 1996). The isothermal wind starts with an initial velocity $v(R_{\rm r}^{\rm c}) = 3\ {\rm km\,s^{-1}}$ perpendicular to this sphere. The mass-loss rate, $\dot{M}_{\rm r}$, is taken from Kenyon & Fernandez-Castro (1987), the stellar masses and orbital period are from Schild et al. (1996). The constant gas temperature, $T_{\rm e}$, was set to a value typical for the electron temperature in the ionized nebula of symbiotic binaries. For the average mass per nucleus, $\mu$, we assume solar composition, where hydrogen is fully ionized.

**Table 2.** Our model parameters. The subscript r refers to the M-giant, h to the accreting whitedwarf. The radii correspond to numerical and not physical surfaces.

| | |
|---|---|
| Mass $M_{\rm r}$ [${\rm M}_\odot$] | 1.6 |
| Radius $R_{\rm r}^{\rm c}$ [${\rm R}_\odot$] | 150 |
| Orbital velocity $v_{\rm r}$ [km/s] | 8.8 |
| Mass-loss $\dot{M}_{\rm r}$ [${\rm M}_\odot$/yr] | $10^{-7}$ |
| Initial velocity $v(R_{\rm r}^{\rm c})$ [km/s] | 3 |
| Mass $M_{\rm h}$ [${\rm M}_\odot$] | 0.48 |
| Radius $R_{\rm h}^{\rm c}$ [${\rm R}_\odot$] | 8 |
| Orbital velocity $v_{\rm h}$ [km/s] | 29 |
| Binary separation $s$ [${\rm R}_\odot$] | 275 |
| Orbital period $P$ [d] | 370.3 |
| Gas temperature $T$ [K] | 10 000 |
| Mass per nuclei $\mu$ [amu] | 0.6 |

### *5.2. Hydrodynamic code*

We solve the adiabatic 3D Euler equations employing, $\gamma = 1$ which corresponds to the isothermal case. For this we use the AMRCART code, described in Walder & Folini (2000)[1]. For our simulation we work in a fixed frame of reference. AMRCART combines the adaptive mesh refinement algorithm of Berger (1985) with the high-resolution finite volume integrator of Colella (1990). The numerical method is therefore very similar to that of Ruffert (1996). It is, however, different from the SPH-method used by Theuns & Jorissen (1993) and Mastrodemos & Morris (1998). A comparison made by Walder (1997) confirms that the two different methods give similar results. Even with the adaptive mesh it is beyond present computer resources to resolve the white dwarf with the numerical grid. We have chosen a sphere of radius $R_{\rm h}^{\rm c} = 8\ {\rm R}_\odot$, into which the material is accreted. Along the accreting sphere fully absorbing boundary conditions were applied. These are the same boundary conditions as used by Ruffert (1996). They implicitly assume that the flow between the sphere and the surface of the white dwarf has no influence on the flow outside of the sphere and through the sphere.

### *5.3. Results of the model calculation*

The resulting density and velocity distribution in the orbital plane is shown in Figs. 4 and 5.

The most striking feature in Fig. 4 is the accretion wake, an elongated region of highly increased density. The accretion wake is limited by an inner and an outer shock front, behind which the density steeply rises, leading to an inner and an outer high density ridge. Due to geometrical rarefaction and wind acceleration, the inner ridge is much denser than the outer ridge. In addition, the inner high density ridge close to the accretor extends along an almost straight line (Fig. 5). This geometry, together with the high densities along the inner ridge, leads to the strongly enhanced column density at $\phi_{\rm max} \approx 0.7$ in Fig. 6,

[1] AMRCART is available on request from walder@astro.phys.ethz.ch

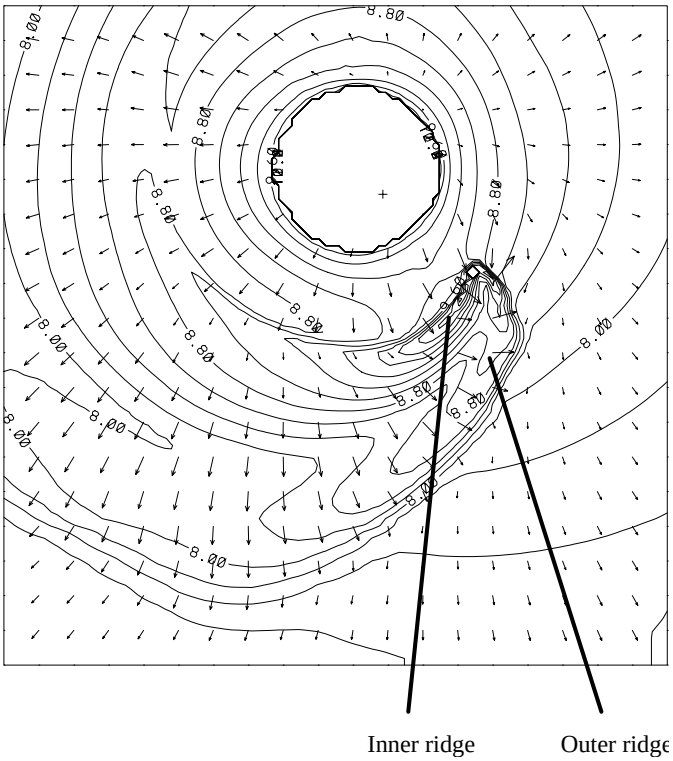


**Fig. 4.** Hydrodynamical simulation for the RW Hya system. Density (logarithmic) and projected velocity distribution in the orbital plane. Densities are given by contour lines, velocities by arrows. In the upper panel arrows of $1\ \mathrm{mm}$ correspond to a velocity of $20\ \mathrm{km\,s^{-1}}$. The system rotates anti-clockwise. The center of mass is marked with a cross, The accretor is marked with a small circle.

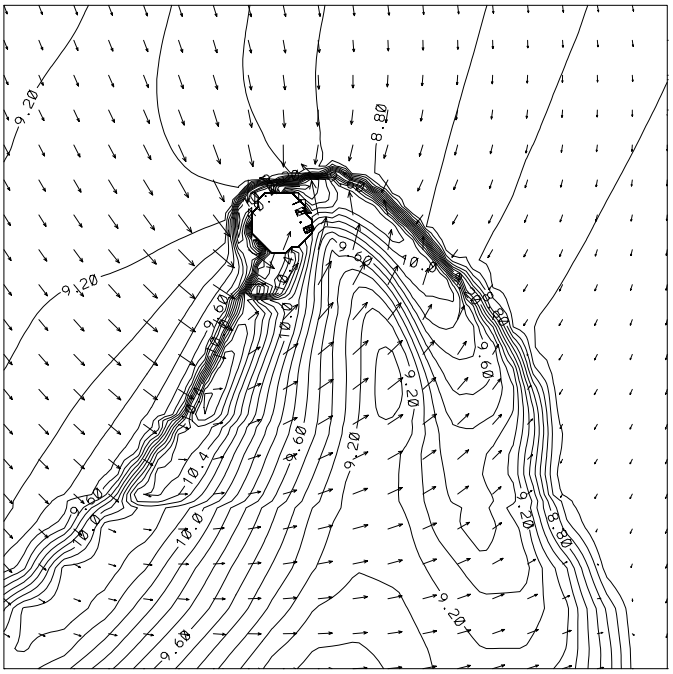

**Fig. 5.** Enlargement of Fig. 4, showing both high density ridges in the neighbourhood of the accretor. The circle corresponds to the numerical boundary of the accretor.

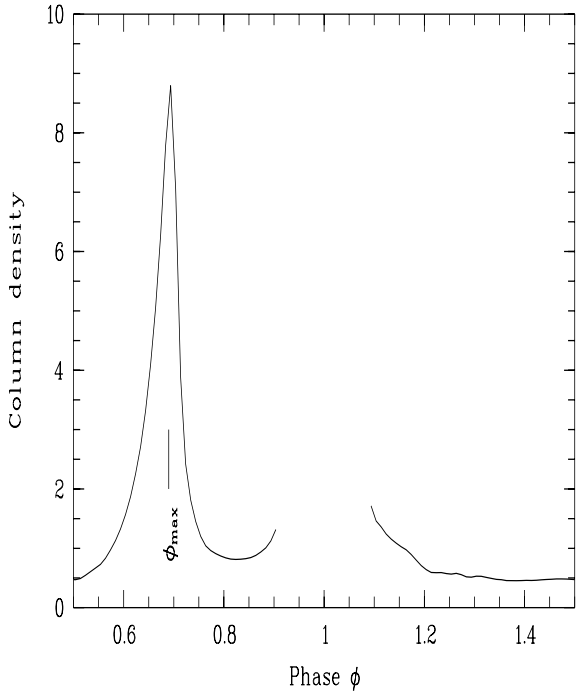


**Fig. 6.** Column densities on the line of sight to the accretor, in units of $10^{23}\ \mathrm{cm^{-2}}$. The densities are calculated from our numerical simulation. The gap around $\phi = 0$ is due to the M-giant's photospheric eclipse.

with peak column density $\approx 9 \cdot 10^{23}\ \mathrm{cm^{-2}}$. About $75\%$ of this maximum column density arises from matter closer than $70\ \mathrm{R_\odot}$ to the accretor. Contrary to the inner high density ridge, the outer ridge is strongly curved. Because of this, and due to smaller densities, the outer ridge does not lead to high column densities in Fig. 6. In Fig. 6 we show the column density towards the accretor as a function of orbital phase. There, the width at half of the maximum column density due to the inner high density ridge is $\Delta\phi \approx 0.05$. There the ionizing photons from the white dwarf radiation field can no longer compensate for the much increased recombination of ionized hydrogen, and a neutral region can form, with peak column densities of neutral hydrogen of the order of $10^{23}\ \mathrm{cm^{-2}}$, which is of the order of the observed column density of neutral hydrogen at $\phi = 0.78$. It is this neutral region along the inner high density ridge which we associate with the observed high column density close to quadrature.

We find that the position of both ridges is stable. From our simulation we get a stable accretion rate of $\approx 6 \cdot 10^{-9}\ \mathrm{M_\odot/yr}$. Thus $6\%$ of the M-giant wind is captured by the accretor. This value is comparable to what has been found by Mastrodemos & Morris (1998) for their Model 3. The accretion efficiency is thus much smaller than, for Bondi-Hoyle accretion.

Between the numerical boundary of the accretor at $R_\mathrm{h}^\mathrm{c} = 8\ \mathrm{R_\odot}$ and $r \approx 10\ \mathrm{R_\odot}$, in the plane of the orbit, we find an almost circular flow around the accretor. We cannot decide whether an accretion disk would form around the accretor if a smaller calculation boundary were chosen. We expect that the formation

of an accretion disk would not significantly influence the shape of the accretion wake.

## 6. Conclusions

In UV spectra of RW Hya, taken around $\phi = 0.78$, there is evidence for a high column density of neutral hydrogen along the line of sight to the hot white dwarf. We have demonstrated that this observation can qualitatively be interpreted in terms of a wind accretion model with an associated accretion wake. If the high column density is indeed due to accretion, we have found the first direct observational detection of wind accretion onto a white dwarf in a detached binary system.

Our wind accretion simulation shows a pronounced peak in column density in the line of sight to the accretor for a relatively short phase interval. This peak is due to the high density ridge behind the inner shock of the accretion wake. In our model the height of the peak, i.e. the column density, depends on the mass-loss rate of the M-giant. The high densities increase the recombination rate, and lead to a narrow cone of neutral hydrogen. This cone of neutral hydrogen leads to Rayleigh attenuation if viewed from a favourable angle. The amount of neutral hydrogen formed in the wake strongly depends on the luminosity of the accretor and also on the density structure of the unresolved area inside the computational radius of the accretor $R_h^c = 8\,\mathrm{R}_\odot$. If about half of the total column density of hydrogen through the wake is neutral hydrogen, the width of the wake of neutral hydrogen would be in good agreement with the observed UV-light curve.

In our model, the orbital phase $\phi_{\max}$ at which the line of sight to the accretor passes trough the inner ridge depends on the ratio of the unperturbed wind velocity in the neighbourhood of the accretor to the orbital velocity of the accretor. Negligible orbital velocity imply $\phi_{\max} \approx 0.50$, whereas a large orbital velocity results in $\phi_{\max} \approx 0.75$. In our model the unperturbed wind velocity at the position of the accretor is $\approx 18\ \mathrm{km\,s^{-1}}$, which is $\approx 2/3$ of the orbital velocity, leading to $\phi_{\max} \approx 0.7$. If the observed high column density of neutral hydrogen at $\phi = 0.78$ is indeed due to an accretion wake, this indicates that the unperturbed M-giant wind velocity at the distance of the white dwarf is smaller than $\approx 18\ \mathrm{km\,s^{-1}}$.

Our interpretation of the occultation around quadrature assumes that the white dwarf has no wind and no radiation field, of sufficient strength to prevent accretion. This assumption cannot be verified with current observations. A wind, as predicted by the theory of radiation driven winds, would not be detected in the HST spectra analyzed in Sect. 4, but could still prevent accretion. However, the colliding wind model 'weak' ($r/s = 0.3$) of Walder (1998), which is representative for the colliding wind model predicted by the wind momentum-luminosity relation, does not lead to an isolated high column density at $\phi \approx 0.75$.

According to the evolutionary model for a $1.5\ \mathrm{M}_\odot$ post-AGB single star (Vassiliadis & Wood 1994) the time for a white dwarf to cool from $L \approx 1000\ \mathrm{L}_\odot$ down to $L \approx 50\ \mathrm{L}_\odot$ is $\approx 100\,000$ years. This is short compared to the time it takes for an early type $1.5\ \mathrm{M}_\odot$ M-giant to become a planetary nebula. Thus, it is likely that the white dwarf was previously less luminous than it is now in its symbiotic binary phase. We expect that the white dwarf in a detached binary system has accreted hydrogen and helium rich M-giant matter in the pre-symbiotic phase. If the white dwarf enters the symbiotic phase, it then has a hydrogen and helium rich surface layer. For such a white dwarf which undergoes mass-loss at $< 10^{-10}\ \mathrm{M}_\odot/\mathrm{yr}$, it is likely that hydrogen and helium in the wind decouple from the metallic ions (Springmann & Pauldrach 1992, Porter & Skouza 1999). In this case the metallic ions can freely accelerate, leaving hydrogen and helium with no further acceleration. If this happens before escape velocity is reached, hydrogen and helium will fall back onto the white dwarf (Porter & Skouza 1999). This leads to a drastic decrease of the hot wind momentum, making it unlikely that the hot wind can prevent accretion. The white dwarf radiation field will also act only upon the in-falling metallic ions in the M-giant wind, with little pressure on the in-falling hydrogen and helium ions. To put stringent upper limit on the mass-loss rate of the white dwarf, new high resolution, high signal to noise UV spectra are needed.

The interplay of accretion and nova-like outbursts in symbiotic systems is an interesting but unsolved question. Since the beginning of the $20^{\mathrm{th}}$ century neither a nova-like outburst, nor any Z Andromeda type activity has been recorded for RW Hya. Spectroscopic and photometric variability is strictly periodic with the orbital period, indicating that it arises from viewing angle effects alone. RW Hya thus belongs to the class of very stable symbiotic binary systems. It appears to be in a quiet stage which is compatible with either a post-outburst plateau luminosity phase, or burning of the accreted hydrogen under steady-state conditions (Sion & Starrfield 1994). The accretion rate of $\approx 6 \cdot 10^{-9}\ \mathrm{M}_\odot/\mathrm{yr}$ in our simulation is sufficient to power the hot component via steady-state thermonuclear burning The total nuclear-burning luminosity of $500\ \mathrm{L}_\odot$ falls in the range of hot component luminosities derived from observations (Kenyon & Mikolajewska 1995; Schild at al. 1996), but one has to keep in mind that the conditions for steady-state burning on a low-mass hot white dwarf strongly depend on its stellar parameters (Sion & Starrfield 1994).

*Acknowledgements.* We thank Ed Sion for discussions on the evolutionary stage of the white dwarf in RW Hya and the referee Dr. Joanna Mikolajewska for clarifying comments on the manuscript. TD acknowledges financial support from the Swiss National Science Foundation.

## References

Ahmad I.A., Parsons S.B., 1985, ApJ 299, L33
Ahmad I.A., 1986, ApJ 301, 275
Ahmad I.A., 1989, ApJ 338, 1011
Berger M.J., 1985, Lectures in Applied Mathematics 22, 31
Bisikalo D.V., Boyarchuk A.A., Kuznetsov O.A., Popov Y.P, Chechetkin V.M, 1995, Astr. Reports 39, 325
Bondi H., Hyole F., 1944, MNRAS 104, 273
Colella P., 1990, J. Comp. Phys. 87, 171
Chapman R.D., 1981, ApJ 248, 1043

Danchi W.C., Bester M., Degiacomi C.G., Greenhill L.J., Townes C.H., 1994, AJ 107, 1469
Dumm T., Schmutz W., Schild H., Nussbaumer H., 1999, A&A 349, 169
Eaton J.A., 1994, AJ 107, 729
Feldmeier A., Anzer U., Börner G., Nagase F., 1996, A&A 311, 793
Howarth I.D., Prinja R.K., 1989, ApJS 69, 527
Hoyle F., Lyttleton R.A., 1939, Proc. Camb. Phil. Soc., 35, 405
Jackson J.C., 1975, MNRAS 172, 483
Kaper L., Hammerschlag-Hensberge G., Zuiderwijk E.J., 1994, A&A 289, 846
Kenyon S.J., Fernandez-Castro T., 1987, ApJ 316, 427
Kenyon S.J., Mikolajewska J., 1995, AJ 110, 391
Kudritzki R.P., 1998, In: Livio M. (ed.) Proceedings of STScI Conference, Cambridge University
Mastrodemos N., Morris M., 1998, ApJ 497, 303
Nussbaumer H., Vogel M., 1996, A&A 307, 470
Nussbaumer H., Dumm T., 1997, A&A 323, 387
Nussbaumer H., Schmutz W., Vogel M., 1995, A&A 293, L13
Pounds K.A., Cooke B.A., Ricketts M.J., Turner M.J., Elvis M., 1975, MNRAS 172, 473
Porter J.M., Skouza B.A., 1999, A&A 344, 205
Ruffert M., 1996, A&A 311, 817
Sion E.M., Starrfield S.G., 1994, AJ 421, 261
Schild H., Mürset U., Schmutz W., 1996, A&A 306, 477
Schmutz W., 1996, In: Benvenuti P., et al. (eds.) Science with HST-II, Proc STScI/ST-ECF Workshop, p. 366
Shore S.N., Aufdenberg J.P., 1993, ApJ 416, 355
Springmann U.W.E., Pauldrach A.W.A., 1992, A&A 296, 761
Theuns T., Jorissen A., 1993, MNRAS 265, 946
Theuns T., Boffin H.M.J, Jorissen A., 1996, MNRAS 280, 1264
Vassiliadis E., Wood P.R., 1994, ApJS 92, 125
Vogel M., 1991, A&A 249, 173
Vogel M., 1993, A&A 274, L21
Walder R., Folini D., 2000, to appear in: Lamers H.J.G.L.M., Sapar A. (eds.) Thermal and Ionization Aspects of Flows from Hot Stars: Observations and Theory. ASP Conference Series
Walder R., 1997, In: Wickramasinghe D.T., Ferrario L., Bicknell G.V. (eds.) Accretion phenomena and related outflows. IAU Colloquium No. 163, ASP Conference Series No. 121, p. 822
Walder R., 1998, Ap&SS 260, 243
Watson M.G., Griffiths R.E., 1977, MNRAS 178, 513